World Journal of Microbiology and Biotechnology (2021) 37:9
https://doi.org/10.1007/s11274-020-02972-6

ORIGINAL PAPER

Optimization of theoretical maximal quantity of cells to immobilize on solid supports in the rational design of immobilized derivatives strategy

Freddy Castillo-Alfonso[1,6] · Marcia M. Rojas[2] · Irina Salgado-Bernal[2] · María E. Carballo[2] · Roberto Olivares-Hernández[4] · Jorge González-Bacerio[1,3] · José M. Guisán[5] · Alberto del Monte-Martínez[1]

Received: 1 October 2020 / Accepted: 29 November 2020 / Published online: 4 January 2021

Abstract

Current worldwide challenges are to increase the food production and decrease the environmental contamination by industrial emissions. For this, bacteria can produce plant growth promoter phytohormones and mediate the bioremediation of sewage by heavy metals removal. We developed a Rational Design of Immobilized Derivatives (RDID) strategy, applicable for protein, spore and cell immobilization and implemented in the $RDID_{1.0}$ software. In this work, we propose new algorithms to optimize the theoretical maximal quantity of cells to immobilize (tMQ_{Cell}) on solid supports, implemented in the $RDID_{Cell}$ software. The main modifications to the preexisting algorithms are related to the sphere packing theory and exclusive immobilization on the support surface. We experimentally validated the new tMQ_{Cell} parameter by electrostatic immobilization of ten microbial strains on AMBERJET® 4200 Cl^- porous solid support. All predicted tMQ_{Cell} match the practical maximal quantity of cells to immobilize with a 10% confidence. The values predicted by the $RDID_{Cell}$ software are more accurate than the values predicted by the $RDID_{1.0}$ software. 3-indolacetic acid (IAA) production by one bacterial immobilized derivative was higher (~ 2.6 µg IAA-like indoles/10^8 cells) than that of the cell suspension (1.5 µg IAA-like indoles/10^8 cells), and higher than the tryptophan amount added as indole precursor. Another bacterial immobilized derivative was more active (22 µg Cr(III)/10^8

Electronic supplementary material The online version of this article (https://doi.org/10.1007/s11274-020-02972-6) contains supplementary material, which is available to authorized users.

✉ Jorge González-Bacerio
jogoba@fbio.uh.cu

✉ Alberto del Monte-Martínez
adelmonte@fbio.uh.cu

Freddy Castillo-Alfonso
fcastillo.alfonso@gmail.com

Marcia M. Rojas
marcia@fbio.uh.cu

Irina Salgado-Bernal
irina@fbio.uh.cu

María E. Carballo
mecarballo@fbio.uh.cu

Roberto Olivares-Hernández
rolivares@correo.cua.uam.mx

José M. Guisán
jmguisan@icp.csic.es

[1] Centro de Estudio de Proteínas, Universidad de La Habana, Calle 25, #455, e/J e I, Vedado, 10400 Havana, Cuba

[2] Departamento de Microbiología y Virología, Universidad de La Habana, Calle 25, #455, e/J e I, Vedado, 10400 Havana, Cuba

[3] Departamento de Bioquímica, Facultad de Biología, Universidad de La Habana, Calle 25, #455, e/J e I, Vedado, 10400 Havana, Cuba

[4] Universidad Autónoma Metropolitana, Unidad Cuajimalpa. Av. Vasco de Quiroga 4871, Col. Santa Fe Cuajimalpa, Delegación Cuajimalpa, 05348 Mexico, Mexico

[5] Departamento de Biocatálisis, Instituto de Catálisis y Petroleoquímica, Consejo Superior de Investigaciones Científicas (CSIC), Campus Cantoblanco, 28049 Madrid, Spain

[6] Present Address: Posgrado en Ciencias Naturales e Ingeniería, Universidad Autónoma Metropolitana, Unidad Cuajimalpa. Av. Vasco de Quiroga 4871, Col. Santa Fe Cuajimalpa, Delegación Cuajimalpa, 05348 Mexico, Mexico

cells) than the resuspended cells (14.5 µg Cr(III)/10^8 cells) in bioconversion of Cr(VI) to Cr(III). Optimized RDID strategy can be used to synthesize bacterial immobilized derivatives with useful biotechnological applications.

Graphic Abstract

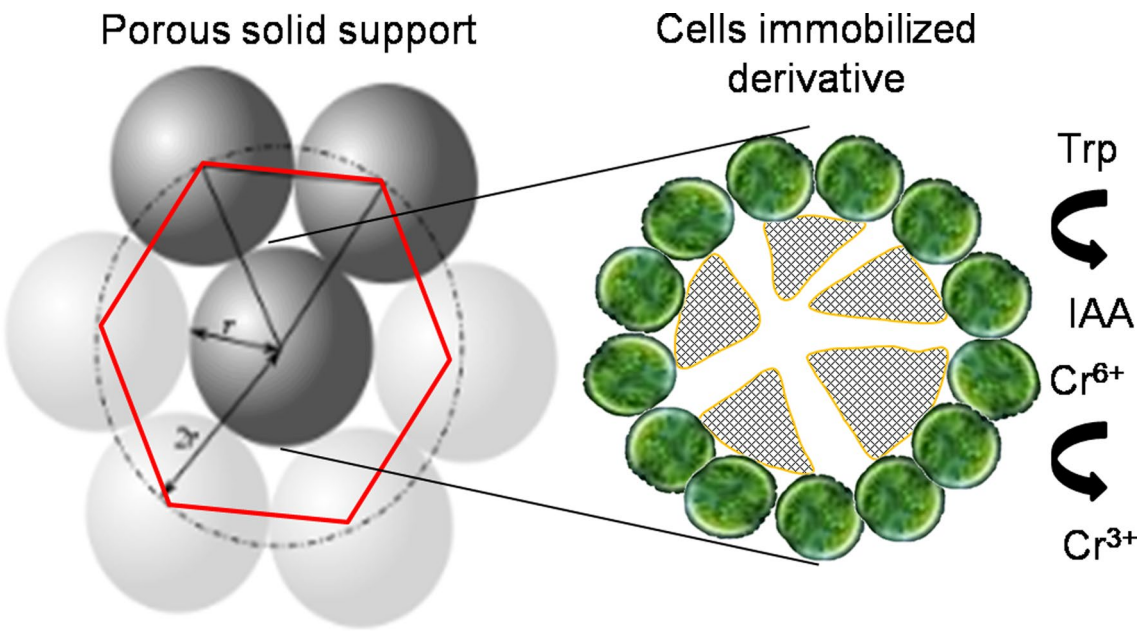

Keywords AMBERJET® 4200 Cl^- porous solid support · Bacterial Cr(VI) removal · Bacterial IAA production · Cell electrostatic immobilization · Rational design of immobilized derivatives strategy · Theoretical maximal quantity of cells to immobilize

Introduction

Cells are very useful biocatalysts on industrial processes (Beshay et al. 2002; Kwon et al. 2011; Sethi et al. 2013; Eş et al. 2018). Cells immobilization is a process of unquestionable biotechnological relevance and one of their more known advantages is the catalyst reusing (Guisán 2006; Kumar and Vats 2010). The most used cell immobilization methods are entrapment and adsorption on supports (Verstrepen et al. 2003). Among the products industrially obtained by immobilized microorganisms are enzymes, ethanol, phytohormones and antibiotics (Steffan et al. 2005; Sethi et al. 2013; Zhang et al. 2019). Cells immobilization by electrostatic interactions with ionic exchange supports has emerged as an attractive immobilization strategy, due to its simplicity (Guisán 2013).

A current worldwide challenge is to increase the food production, improving the crops growth (Davis et al. 2017). Plant growth promoting bacteria (PGPB) synthesize the auxin indole-3-acetic acid (IAA), which can stimulate the development of the radical system and the general host-plant growth (Pini et al. 2011; Khandaker et al. 2018). There are two pathways in bacteria to produce IAA: tryptophan-dependent and tryptophan-independent pathways (Duca et al. 2014; Zhang et al. 2019). Another current challenge is to decrease the environmental contamination with heavy metals due to industrial emissions (Nazhmetdinova et al. 2018). Microbial bioremediation is a promising alternative, due to economical, sensitivity and specificity issues, as well as the structural, physiological and metabolic diversity of microorganisms (Cristani et al. 2012; Labra-Cardón et al. 2012; Zinicovscaia 2012; Fosso-Kankeu et al. 2014).

Cell immobilization is visualized as an attractive alternative to board IAA production and bioremediation. As a useful tool in this field, we developed a Rational Design of Immobilized Derivatives (RDID) strategy, applicable for protein, spore and cell immobilization (del Monte et al. 2010, 2013; del Monte-Martínez et al. 2014, 2017, 2018, 2019) and implemented in the $RDID_{1.0}$ software. This strategy is directed to predict the behavior of the immobilized derivative before its synthesis, using mathematic algorithms and bioinformatics tools, and select the optimal conditions for its synthesis (del Monte-Martínez and Cutiño-Avila 2012). In this work, we propose new algorithms to optimize the theoretical maximal quantity of cells to immobilize per support g (tMQ_{Cell}) on solid supports, implemented in the

$RDID_{Cell}$ software. We experimentally validated the new tMQ_{Cell} parameter by electrostatic immobilization of ten microbial strains on AMBERJET® 4200 Cl^- porous solid support, and used two immobilized derivatives for biotechnological applications, such as IAA production and hexavalent chrome (Cr(VI)) bioremediation.

Materials and methods

Microorganisms

Eight bacterial strains (Gram-positive and Gram-negative) were used: *Escherichia coli* BL21, *Micrococcus luteus* ATCC 10240, *Pseudomonas aureginosa* ATCC 27853, *Bacillus* sp. strains RC9 and RC15 (originally isolated from coffea rhizosphere), *Bacillus wiedmannii* TAN-125 and strains TAN-113 and TAN-311 (originally isolated from rhizosphere of the hydrophyte plant *Typha dominguensis*). In addition, two yeast strains were used: *Pichia pastoris* KM71H and *Saccharomyces cerevisiae* ATCC 9763. All these strains were obtained from the microbial culture collection, Faculty of Biology, University of Havana, Cuba. The morphological characteristics of these strains are shown in Table S1.

Culture media

For bacteria, the Nutrient Broth medium (Sigma-Aldrich, MO, USA) was used. For yeast, the YPD medium (Sigma-Aldrich, MO, USA) was used (20 g/L yeast extract, 20 g/L peptone, 10 g/L dextrose). Both solid media were prepared adding 1.5% agar (Sigma-Aldrich, MO, USA). For bioconversion and bioremediation assays the minimal medium for *Bacillus* (Department of Microbiology and Virology, Faculty of Biology, University of Havana) was used (10 g/L sucrose, 2.5 g/L KH_2PO_4, 1 g/L $(NH_4)_2HPO_4$, 0.2 g/L $MgSO_4{\cdot}7H_2O$, 0.01 g/L $FeSO_4{\cdot}7H_2O$, 0.007 g/L $MnSO_4{\cdot}H_2O$).

Computational methodology

Structural and functional characteristics of microbial species used in this work were obtained from: Model Organism Databases - National Human Genome Research Institute (https://www.genome.gov/10001837/model-organism-databases/), Evomining (http://codigof.mx/evomining), Celldesigner (http://www.celldesigner.org/features/features41B.html), and Mining PubMed for relationships (http://www.chilibot.net/). As part of the RDID strategy, mathematic algorithms to calculate the tMQ_{Cell} parameter were redesigned. Building of the $RDID_{Cell}$ software was performed in Python language version 3.5 (Python Software Foundation; http://www.python.org/).

Obtainment of cell biomasses

Purity of used strains to obtain the cell biomasses was tested by microscopic observation (Novel Optics, Nanjing, China), applying the Gram staining for bacterial strains and the Nigrosine staining for yeast strains (Madigan et al. 2012). Cultural characteristics of bacterial and yeast strains were observed by streaking in 90 mm plates (Sigma-Aldrich, MO, USA) with agar-nutrient or agar-YPD media, respectively, incubating at 30 °C, pH 7.0 for 24 h, or 28 °C, pH 5.6 for 72 h, respectively, and observing with stereomicroscope (Novel Optics, Nanjing, China). Obtainment of bacterial and yeast biomasses was performed inoculating a colony in 50 mL Nutrient Broth or YPD media and incubating in the same previous conditions.

Cell diameter measurement

Cell diameter measurement (20 cells/strain) was performed in microphotographs obtained with an optic microscope (Motic, Novel Optics, Nanjing, China), using a coupled Canon camera (Canon, Tokyo, Japan), and processed by the software Motic Image 2000 (https://www.microscopeworld.com/t-software.aspx). As type microphotograph was used one obtained from the strain *P. aeruginosa* ATCC 27853. Bacteria and yeast were submitted to Gram and Nigrosine staining, respectively. For rod-shaped bacteria, the cell diameter was the average between the lowest and highest diameters.

Preparation of cell suspensions

For experimental validation of tMQ_{Cell}, microbial suspensions were prepared in 0.1 M imidazole–HCl buffer, pH 7.0 (immobilization buffer), adjusting the cell concentration at different values (using the McFarland scale (NCCLS, 2005)), taking as a reference the tMQ_{Cell}. For bioconversion and bioremediation assays, microbial suspensions were prepared in minimal medium for *Bacillus*, pH 7.0. For cell count (by triplicate), microbial suspensions were prepared in 0.85% NaCl, at 10^8 cells/mL, according to tube 0.5 of the McFarland scale, and quantification was performed by microscopic count using Neubauer chamber.

Immobilization of live microbial cells on the AMBERJET® 4200 Cl^- porous solid support

Immobilization of the ten microbial strains by ionic adsorption on AMBERJET® 4200 Cl^- porous solid support (Rhom & Haas, PA, USA) was performed according to del Monte et al. (2013). One g of support (pre-washed several times with distilled water) was mixed with 5 mL cell suspension in 0.1 M imidazole–HCl buffer, pH 7.0. The mixture was

submitted to orbital shaking at 200 rpm and 30 °C for 24 h. The immobilized derivative was collected by decantation, washed three times with the same buffer and kept at 4 °C. For tMQ_{Cell} experimental validation, a cell load study was performed with ten different cell concentrations for each strain and the immobilization isotherms were obtained. Immobilization was controlled by the parameter differential immobilization grade (cells) (*diff.* IG_{Cell}; expressed on cell number/support g) according to del Monte-Martínez et al. (2012) for proteins. The experimental parameter practical maximal quantity of cells to immobilize (pMQ_{Cell}) was calculated from the obtained *diff.* IG_{Cell} values according to del Monte-Martínez et al. (2018) for proteins.

Bioconversion assay for IAA production

Bioconversion assays for IAA production were performed with the cell suspension of *Bacillus* sp. RC15 strain, and its resultant immobilized derivative, in minimal medium for *Bacillus*, pH 7.0, supplemented with 20 µg/mL tryptophan (final volume: 5 mL). For the immobilized derivative, one support g was used with a cellular load corresponding to pMQ_{Cell}. Bioconversion assays were performed with shaking at 30 °C for 24 h. After this time, the supernatant was collected and kept at 4 °C for product quantification. As negative control, one support g without immobilized cells was used.

IAA-like indoles were quantified (by triplicate) by the colorimetric method using the Salkowski reagent (Glickmann and Dessaux 1995). Five-hundred µL supernatant were mixed with 500 µL Salkowski reagent (12 g of anhydrous $FeCl_3$ in 1 L of 7.9 M H_2SO_4). This mixture was incubated in the dark for 30 min and the reaction was finished by light exposition. Sample absorbance was measured at 530 nm. A standard curve of IAA was prepared (Fig. S1). IAA specific productivity (*SpecProd*) was calculated as the ratio between produced IAA concentration and cell concentration.

IAA was identified and semi-quantified by thin layer chromatography (TLC) on silica gel plates (20 × 10 cm; Merck, Darmstadt, Germany). Applications (5 µL supernatants or standards) were performed at 1.5 cm from the plate base, 1 cm from the left and right borders, and separated from each other by 1 cm. One mg/mL tryptophan and IAA standards were applied. Mobile phase was isopropanol:ammonia:water (10:1:1, v/v/v) (Héctor et al. 1995; del Monte-Martínez et al. 1999). Runs were performed until the solvent front reached 1 cm before the plate superior border. After 10 min drying, revealing was performed by exposition to the UV light at 258 nm. Chromatographic plates were photographed with a Canon camera (Canon, Tokyo, Japan) and images were processed by the ImageJ software version 2.0. Tryptophan and IAA standard curves were prepared applying 5, 10, 15, 20 and 50 µg/mL (Fig. S2).

Bioremediation assays for Cr(VI) removal

Bioremediation assays for Cr(VI) removal were performed with the cell suspension of *Bacillus wiedmannii* TAN-125, and its resultant immobilized derivative, in minimal medium for *Bacillus*, pH 7.0, supplemented with potassium dichromate ($K_2Cr_2O_7$) (final volume: 5 mL). For the immobilized derivative, one support g was used with a cellular load corresponding to pMQ_{Cell}.

Since the AMBERJET® 4200 Cl^- support is a porous solid industrially used as anion exchanger (Wassel et al. 2013), firstly was established its ability to adsorb the $(Cr_2O_7)^{2-}$ anion. For this, one support g was mixed with different amounts of $K_2Cr_2O_7$ to build the adsorption isotherm (Fig. S3). Assays were performed by triplicate at pH 7.0 and 25 °C. For this, the samples absorbance at 365.6 nm was determined. A $(Cr_2O_7)^{2-}$ standard curve was built (Fig. S4). The differential adsorption degree (*diff. AD*) parameter was determined according to the equation:

$$diff.AD = \left(\text{initial quantity } \left(Cr_2O_7\right)^{2-}/\text{support g}\right) - \left(\sum \text{quantity } \left(Cr_2O_7\right)^{2-}(\text{filtrates and washes})/\text{support g}\right)$$

When the condition

$$\left[diff.AD\left(i\left(Cr_2O_7\right)^{2-}\text{concentration}\right) - diff.AD\left(i+1\left(Cr_2O_7\right)^{2-}\text{concentration}\right)\right]/diff.AD\left(i\left(Cr_2O_7\right)^{2-}\text{concentration}\right) < 0.03$$

was accomplished, then the total *diff. AD* was reached (Fig. S3). Afterward, the support exchanger sites were blocked with equivalent quantities of $(PO_4)^{3-}$ anion. For this, the support was treated with K_2HPO_4 (150×10^3 µg $(PO_4)^{3-}$/support g) before cell immobilization.

Bioremediation assays were performed with shaking at 30 °C for 24 h. After this time, the supernatant was collected and kept at 4 °C for product quantification. As negative control, one support g without immobilized cells and treated with K_2HPO_4 was used. Samples were analyzed in an atomic absorption spectrometer with air-acetylene flame (AAnalyst 200 AA, PerkinElmer, Waltham, MA, USA), at a wavelength of 357.9 nm. Samples were treated according

to manufacturer instructions for trivalent chrome (Cr(III)) detection. A Cr(III) standard curve was built (Fig. S5).

Statistical analysis

Normal distribution and homogeneity of variances of the experimental data were verified by the Kolmogorov–Smirnov and the Bartlett test, respectively (Snedecor and Cochran 1989). Afterward, an analysis of variance of simple classification was carried out. The means were compared by the Tukey HSD test (Tukey 1949). A level of signification of 0.05 was used. To perform these analyses, the software Statistica (version 8.0; StatSoft Inc. [http://www.statsoft.com]) was used.

Results

Redesign of mathematic algorithms to determine tMQ_{Cell}

In this work, we redesigned the equation to calculate tMQ_{Cell} for cell immobilization. The resultant equation is:

$$tMQ_{Cell} = (SPN \times ASSA) / LIA$$

where *SPN* is the total number of support particles per support g, *ASSA* is the support activated surface area, and *LIA* is the cell or spore area interacting with the support. Redefined *SPN* was recalculated according to:

$$SPN = 5/6\left(V_{h\,supp}/V_{sph}\right)$$

where 5/6 is the correction parameter applied, $V_{h\,supp}$ is the volume occupied by the solvated spheres, experimentally measured, and V_{sph} is one sphere volume ($4/3\pi r^3$).

Since the support pore diameter is much lower than the cell diameter, immobilization only will take place in the support sphere surface, and *ASSA* can be calculated as the sphere surface area ($4\pi r^2$). On the other hand, considering the cell/spore as a sphere, the ligand-support interacting area is the half of the sphere surface area, and it is calculated according to:

$$LIA = 2/\mathrm{pi}(r_{low} \times r_{high})$$

where r_{low} is the cell or spore lowest ratio, and r_{high} is the ligand highest ratio.

Table 1 tMQ_{Cell} predicted by the $RDID_{Cell}$ software for cell immobilization on AMBERJET® 4200 Cl^- support and experimental validation with pMQ_{Cell}

Strain	tMQ_{Cell} ($\times 10^8$ cells/support g)	pMQ_{Cell} ($\times 10^8$ cells/support g)
Micrococcus luteus ATCC 10240	44.2	44.1 ± 0.2
Escherichia coli BL21	6.77	6.74 ± 0.06
Pseudomonas aeruginosa ATCC 27853	2.35	2.32 ± 0.02
Pichia pastoris KM71H	0.44	0.43 ± 0.01
Saccharomyces cerevisiae ATCC 9763	0.32	0.29 ± 0.03
Bacillus sp. RC9	7.07	6.8 ± 0.3
Bacillus sp. RC15	1.78	1.75 ± 0.07
Bacillus sp. TAN-113	1.78	1.82 ± 0.01
Bacillus wiedmannii TAN-125	7.07	6.7 ± 0.4
Bacillus sp. TAN-311	0.99	0.91 ± 0.09

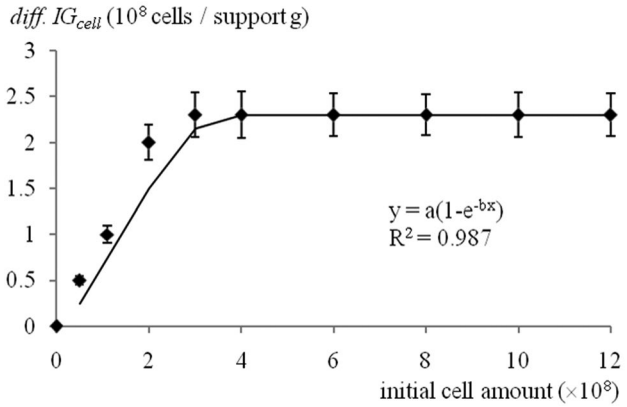

Fig. 1 Immobilization isotherm for electrostatic immobilization of *Pseudomonas aeruginosa* ATCC 27853 on the porous solid support AMBERJET 4200 Cl^-, resultant of the load study. Data are presented as the mean ± standard deviation of three replicates

Determination of tMQ_{Cell} for cell immobilization on porous solid supports and experimental validation with pMQ_{Cell}

tMQ_{Cell} was determined for ten microorganism strains from different species and genera with diverse morphology (Table S1). First, the cell diameters were measured (Table S2). tMQ_{Cell} were determined for the AMBERJET® 4200 Cl^- support (Table 1).

tMQ_{Cell} was experimentally validated with pMQ_{Cell}, resultant of load studies with the ten microbial strains immobilized on the porous solid support AMBERJET® 4200 Cl^- (Table 1). The immobilization isotherm of *P. aeruginosa* ATCC 27853 is shown as an example (Fig. 1); the others can

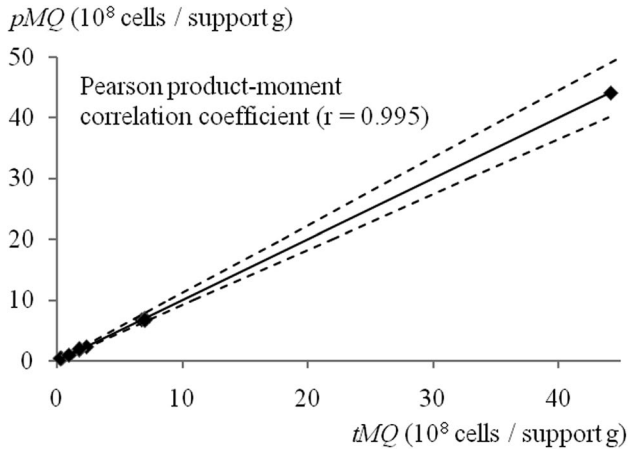

Fig. 2 Correlation between tMQ_{Cell} and pMQ_{Cell} for electrostatic immobilization of ten microbial strains on the porous solid support AMBERJET 4200 Cl^-. Data are presented as the mean ± standard deviation of three replicates. Discontinuous lines: zone inside 10% variability of r

be found in Fig. S6. The comparison between tMQ_{Cell} and pMQ_{Cell} demonstrates the high accuracy degree of predictions (Table 1), quantified by a Pearson product-moment correlation coefficient of 0.995 (Fig. 2).

tMQ_{Cell} predicted by the $RDID_{Cell}$ software was compared with the values predicted by the previous $RDID_{1.0}$ software for the unicellular alga *Scenedesmus obliquus* and the spores of the fungus *Aspergillus niger* J-1 (del Monte et al. 2013; Table 2). This comparison demonstrates that tMQ_{Cell} predicted by the $RDID_{Cell}$ software are more accurate than the values predicted by the $RDID_{1.0}$ software, confirmed by a higher Pearson product-moment correlation coefficient (r = 0.854 *vs.* 0.786) for correlation between tMQ_{Cell} (predicted by $RDID_{Cell}$ *vs.* $RDID_{1.0}$ softwares, respectively) and pMQ_{Cell} for these two ligands (Fig. 3a). When the analysis was performed for the ten strains used in this work plus these two ligands, using the $RDID_{Cell}$ software, r was increased to 0.994 (Fig. 3b).

Application of the RDID strategy to immobilize cells for IAA production

For IAA production, the strain RC15 was selected, maintaining constant the cell amount (resuspended or immobilized) in 1.75×10^8 (pMQ_{Cell}; Table 1). Both cell samples, resuspended and immobilized, were able to produce indoles, being the IAA-like indoles production by the cell suspension equivalent to the tryptophan quantity added as indole precursor (Fig. 4). However, indoles production by the immobilized derivative was significantly higher (~ 2.6 µg IAA-like indoles/10^8 cells) than that of the cell suspension (1.5 µg IAA-like indoles/10^8 cells) and the added tryptophan (Fig. 4).

The mobile phase used in the TLC, performed to identify IAA from other indoles, allowed the separation of IAA and tryptophan standards (Fig. 5). In this manner, we confirmed that *Bacillus* sp. RC15 strain, resuspended and immobilized, produces IAA from tryptophan after 24 h incubation. TLC confirmed that the immobilized derivative produces IAA in excess over the added tryptophan (Table S3).

Application of the RDID strategy to immobilize cells for Cr(VI) removal

For Cr(VI) removal, *Bacillus wiedmannii* TAN-125 was selected, maintaining constant the cell amount (resuspended or immobilized) in 6.7×10^8 (pMQ_{Cell}; Table 1). First, an adsorption study of the $(Cr_2O_7)^{2-}$ anion on the AMBERJET® 4200 Cl^- support was performed. As a result, the total amount of $(Cr_2O_7)^{2-}$ electrostatically adsorbed by one support g was $144.5 \times 10^3 \pm 6.0 \times 10^3$ µg (Fig. S3).

Afterward, 150×10^3 µg $(PO_4)^{3-}$ anion were added to block the support exchanger groups. This treatment was successful, since after it the maximal amount of $(Cr_2O_7)^{2-}$ adsorbed by one support g was only $7.7 \pm 0.5 \times 10^3$ µg, being displaced 136.8×10^3 µg (94.7% of the total). This treatment did not affect the electrostatic immobilization of *Bacillus wiedmannii* TAN-125, since after it the pMQ_{Cell} was reached (data not shown). Resuspended or immobilized cells of the selected strain were able to bioconvert Cr(VI) to Cr(III), but the immobilized derivative was more active, with 22 *vs.* 14.5 µg Cr(III) produced per 10^8 cells (Fig. 6).

Discussion

In this work, we redesigned mathematic algorithms to calculate tMQ_{Cell} for cell immobilization, according to the RDID strategy, to achieve a higher accuracy in its predictive

Table 2 tMQ_{Cell} predicted by the $RDID_{1.0}$ and $RDID_{Cell}$ softwares and experimental validation with pMQ_{Cell}

Microorganism	tMQ_{Cell} $RDID_{1.0}$ ($\times 10^8$ cells/support g)	tMQ_{Cell} $RDID_{Cell}$ ($\times 10^8$ cells/support g)	pMQ_{Cell} ($\times 10^8$ cells/support g)
Scenedesmus obliquus	0.17	0.09	0.052 ± 0.003
Aspergillus niger J-1 (spores)	0.19	0.16	0.151 ± 0.009

tMQ_{Cell} $RDID_{1.0}$ and pMQ_{Cell} values were taken from del Monte et al. (2013)

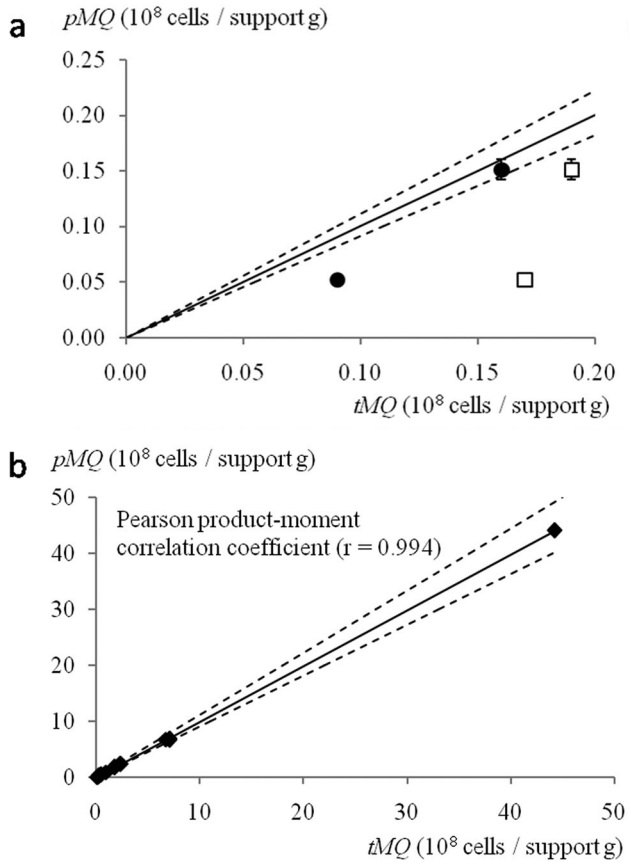

Fig. 3 Correlation between tMQ_{Cell} and pMQ_{Cell}. **a** Correlation between tMQ_{Cell} predicted by the $RDID_{1.0}$ (white squares; del Monte et al. 2013) and $RDID_{Cell}$ (black circles; this work) softwares and pMQ_{Cell} for the alga *Scenedesmus obliquus* and the spores of the fungus *Aspergillus niger* J-1. Pearson product-moment correlation coefficients (r = 0.786 for $RDID_{1.0}$ and 0.854 for $RDID_{Cell}$). **b** Correlation between tMQ_{Cell} predicted by the $RDID_{Cell}$ software and pMQ_{Cell} for these two ligands plus the ten strains used in this work. Data are presented as the mean ± standard deviation of three replicates. Discontinuous lines: zone inside 10% variability of r

ability (del Monte et al. 2010, 2013; del Monte-Martínez and Cutiño-Avila 2012). Redefined *SPN* is calculated as the ratio between the volumes of one solvated support g and one support sphere. In mathematics, the sphere packing analyses are performed considering clusters of spheres with the same size in the tridimensional Euclidean space (Conway and Sloane 2013). In *SPN* equation, 5/6 is the correction parameter applied, considering the regular arrangement with the circle centers disposed in an hexagonal cell with each circle surrounded by other six (Rogers 1947; Aste and Weaire 2000). In cell immobilization, the support pore diameter is much lower than the cell diameter. For example, in the AMBERJET® 4200 Cl^- support, the pore diameter is 10–20 Å (Infante et al. 1996), and the diameter of the littlest cell studied here is 0.5 µm (Medeiros et al. 1971; Hyland et al. 1997).

The measured cell diameters were in the ranges reported in the literature for the collection species (Table S2). Clearly, at higher cell diameter (Table S2), higher *LIA* and lower tMQ_{Cell} (Table 1). The support particle diameter has a high homogeneity (uniformity coefficient = 1.2 (Salager 2007)). When a uniformity coefficient < 3, the material is highly uniform in size (Lambe and Whitman 2007; Orts et al. 2014). For this reason, we assumed that the support particle diameter and *ASSA* are constant for this support, which has a uniform distribution of charged groups.

LIA is also influenced by the microorganism physiological state and the cell wall composition (Kohler et al. 2009). In the cell surface there is a high density of functional groups, represented by proteins and organic acids such as teichoic and lipoteichoic acids (Bera et al. 2007), which contribute with a uniformly distributed high density of negative charges to the cell surface (Weidenmaier et al. 2008). Therefore, cells can establish electrostatic interactions with the quaternary ammonium groups of AMBERJET® 4200

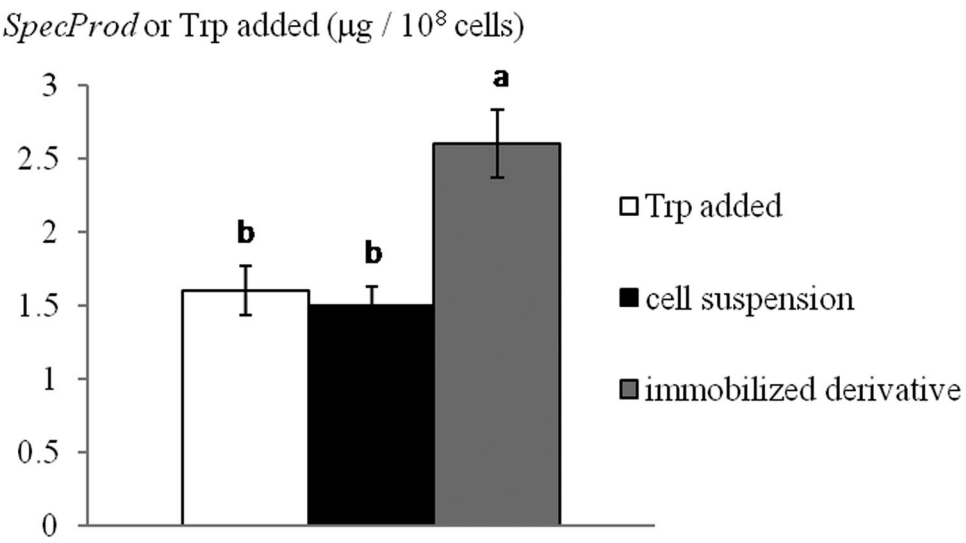

Fig. 4 3-indolacetic acid-like indoles specific productivity of the *Bacillus* sp. RC15 strain, resuspended and electrostatically immobilized on the porous solid support AMBERJET® 4200 Cl^-. Data are presented as the mean ± standard deviation of three replicates. Different letters represent significant differences for p < 0.05. *SpecProd*: specific productivity

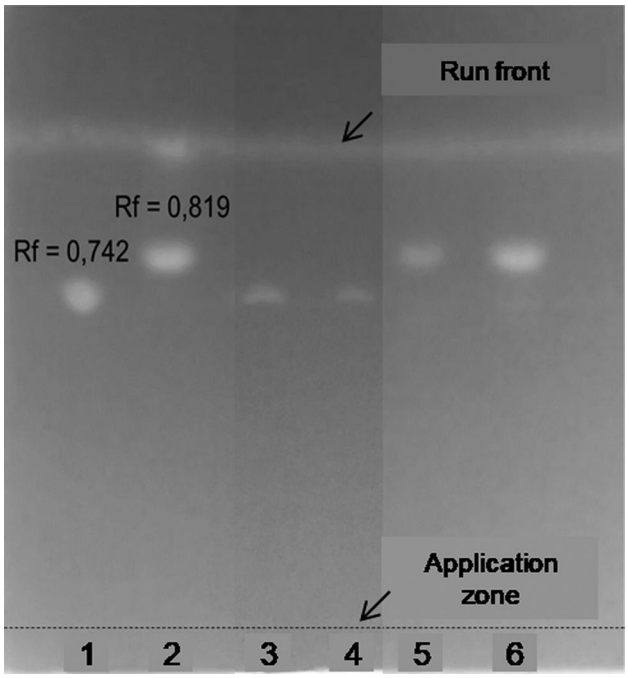

Fig. 5 TLC photograph for 3-indolacetic acid (IAA) production. *1* tryptophan standard. *2* IAA standard. *3* cell suspension of *Bacillus* sp. RC15 strain before the bioconversion process (tryptophan added as precursor). *4* immobilized derivative of RC15 strain before the bioconversion. *5* cells suspension of RC15 strain after 24 h bioconversion. *6* immobilized derivative of RC15 strain after 24 h

Cl^- support. tMQ_{Cell} is very important for cell immobilization. This allows the optimization of the biomass amount that should be used for a given support quantity, making good use of activated surface area. The result obtained after comparing tMQ_{Cell} and pMQ_{Cell} (Table 1; Fig. 2) reinforces the predictive value of the first parameter.

The design of optimal biotransformation processes allows increasing the obtainment efficiency of relevant chemical products, such as drugs, food additives and plant growth promoters, as well as the efficiency in the treatment of industrial emissions (Plou and Sandoval 2012; Sandoval 2012; Castañeda and del Monte-Martínez 2014; Martínez et al. 2014; Menéndez et al. 2014; del Monte-Martínez et al. 2015). The application of the RDID strategy to immobilize cells for bioconversion processes such as IAA production and Cr(VI) removal appears to be a valuable tool. IAA is a very interesting auxin due to its positive effect promoting plant growth (Idris et al. 2007). Its production using bacterial immobilized derivatives contributes with an ecologic agriculture (Rajneesh et al. 2017).

The Salkowski reagent can detect IAA and other indole compounds with auxin activity (Palazon et al. 1995). It is one of the most used methods to detect and semi-quantify IAA due to its easy handling, fast results obtainment and economic feasibility (Torres-Rubio et al. 2000). The higher indoles production by the immobilized derivative, comparing with the cell suspension or the added tryptophan (Fig. 4), suggests that cell immobilization activates the indole synthesis from precursors distinct from tryptophan, which has been reported for IAA production in bacteria (Duca et al. 2014).

This higher bioconversion could be explained by the advantages that immobilization confers. This process can produce a heterogeneous material with favored shaking conditions and nutrient and oxygen transference, showing a higher efficiency than the homogeneous systems. Equally, immobilized derivatives have favorable conditions for cell economy, due to the cell movement restrictions (Willaert 2006). This biocatalyst minimizes diffusional restrictions present in other immobilized systems, as a consequence of cell immobilization in the support surface (Woodward 1988).

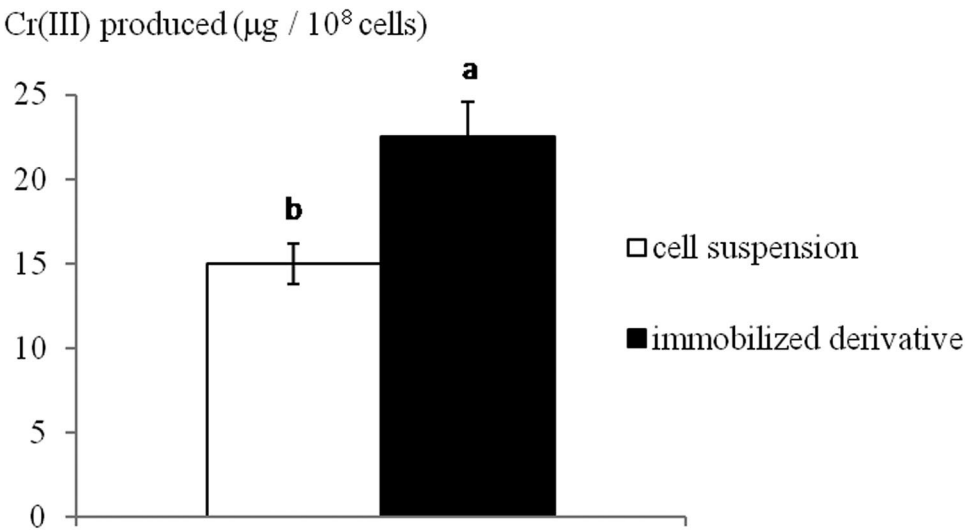

Fig. 6 Cr(VI) removal by its bioconversion to Cr(III) per cell amount. *Bacillus wiedmannii* TAN-125, resuspended and electrostatically immobilized on the porous solid support AMBERJET® 4200 Cl^-, was used. Data are presented as the mean ± standard deviation of three replicates. Different letters represent significant differences for $p < 0.05$

Bacterial immobilized derivatives show relevant applications in microbial bioremediation of sewage (Salgado-Bernal et al. 2015). The adsorption study of the $(Cr_2O_7)^{2-}$ anion on the AMBERJET® 4200 Cl^- support was necessary because the average diameters of the support pore and the anion are 15 Å (Infante et al. 1996) and 1.4 Å (Becerra-Torres et al. 2014), respectively. The ratio between both diameters is 10.7 times, warranting the anion diffusion inside the pores and support adsorption. On the other hand, the average diameter of $(PO_4)^{3-}$ anion is 1.1 Å (Vincent et al. 2006), warranting the effectiveness of the treatment to block the support exchanger groups.

The bioconversion of Cr(VI) to Cr(III) has been previously reported for bacteria, as a resistant mechanism to $(Cr_2O_7)^{2-}$ (Camargo et al. 2003; Ahemad 2014; Thatoi et al. 2014). The advantages of cell immobilization were already mentioned (Woodward 1988; Willaert 2006; Salgado-Bernal et al. 2015). However, we do not discard the existence of other mechanisms for Cr(VI) removal, such as anionic adsorption, reduction-coupled adsorption and bioaccumulation (Cervantes and Campos-García 2007).

In summary, cell immobilization is one of the most used technologies to increase cell operational stability and improve their usage on biotechnological processes. In this work, the RDID strategy was updated for using cells as ligands, by the redesign of algorithms that constitute the software basis. This allowed increase the calculation accuracy and the software's predictive ability. The obtained bacterial immobilized derivatives show important applications on fields such as the microbial bioremediation of sewage, with a positive impact in the environmental improvement, and in production of plant growth promoter phytohormones, directed to contribute with an ecologic agriculture.

Author contribution FCA conducted experiments. MMR, ISB and MEC contributed with conceptualization and methodology. ROH and JMG contributed with resources and supervision. JGB contributed with conceptualization, formal analysis and writing the original draft. AdMM contributed with conceptualization, methodology, supervision, formal analysis, funding acquisition, software and writing the original draft. All authors read and approved the manuscript.

Funding This work was supported by a project associated to the National Program of Basic Sciences (2018-2021), code: P223LH001-093, Cuba.

Data availability All data generated or analyzed during this study are included in this published article (and its electronic supplementary material).

Code availability For access to *RDID*$_{Cell}$ software, please contact with Professor Alberto del Monte-Martínez (adelmonte@fbio.uh.cu).

Compliance with ethical standards

Conflict of interest The authors declare that they have no conflict of interests or competing interests.

References

Ahemad M (2014) Bacterial mechanisms for Cr(VI) resistance and reduction: an overview and recent advances. Folia Microbiol (Praha) 59:321–332. https://doi.org/10.1007/s12223-014-0304-8

Aste T, Weaire D (2000) The pursuit of perfect packing. Institute of Physics Publishing, London

Becerra-Torres SL, Soria-Fregozo C, Jaramillo-Juárez F, Moreno-Hernández-Duque JL (2014) Trastornos a la salud inducidos por cromo y el uso de antioxidantes en su prevención o tratamiento. J Pharm Pharmacog Res 2:19–30

Bera A, Biswas R, Herbert S, Kulauzovic E, Weidenmaier C, Peschel A, Gotz F (2007) Influence of wall teichoic acid on lysozyme resistance in *Staphylococcus aureus*. J Bacteriol 189:280–283. https://doi.org/10.1128/JB.01221-06

Beshay U, Abd-El-Haleem D, Moawad H, Zaki S (2002) Phenol biodegradation by free and immobilized *Acinetobacter*. Biotechnol Lett 24:1295–1297. https://doi.org/10.1023/A:1016222328138

Camargo FA, Bento FM, Okeke BC, Frankenberger WT (2003) Chromate reduction by chromium-resistant bacteria isolated from soils contaminated with dichromate. J Environ Qual 32:1228–1233. https://doi.org/10.2134/jeq2003.1228

Castañeda C, del Monte-Martínez A (2014) Prebióticos y su repercusión en la salud. In: Castañeda C, del Monte-Martínez A (eds) Prebióticos: su obtención y repercusión para la salud. Editorial Mendieta, Quito, pp 35–44

Cervantes C, Campos-García J (2007) Reduction and efflux of chromate by bacteria. In: Nies DH, Silver S (eds) Molecular microbiology of heavy metals. Springer-Verlag, Berlin, pp 407–419

Conway JH, Sloane NJH (2013) Sphere packings, lattices and groups. 3rd edn, vol 290. Springer Science and Business Media, New York

Cristani M, Naccari C, Nostro A, Pizzimenti A, Trombetta D, Pizzimenti F (2012) Possible use of *Serratia marcescens* in toxic metal biosorption (removal). Environ Sci Pollut Res Int 19:161–168. https://doi.org/10.1007/s11356-011-0539-8

Davis KF, Rulli MC, Seveso A, Odorico PD (2017) Increased food production and reduced water use through optimized crop distribution. Nat Geosci 10:919–924. https://doi.org/10.1038/s41561-017-0004-5

del Monte A, Cutiño B, Gil D, Mokarzel L, González J, Pupo M, Chávez MA, Pons T, Díaz J (2010) Rational design strategy on immobilized derivatives synthesis. Their implementation via *RDID*$_{1.0}$ program. Serie Científ Univ Cienc Inf (Cuba) 3:185–202

del Monte A, Cutiño B, Gómez D, Pereda I, Díaz J, Rojas J (2013) Computational mathematic model for the immobilization of cells and proteins on charged solid surfaces by electrostatic interactions. IFMBE Proceeds 33:73–76. https://doi.org/10.1007/978-3-642-21198-0_19

del Monte-Martínez A, Cutiño-Avila BV (2012) Rational design of immobilized lipases and phospholipases. In: Sandoval G (ed) Lipases and phospholipases: methods and protocols, Meth mol biol, vol 861. Humana Press. Springer Science + Business Media, LLC, New York, pp 343–382

del Monte-Martínez A, Laguna A, Pérez N, Héctor E, Maribona RH, Rodríguez R, de Prada F, González R (1999) Detección de un inhibidor de la germinación de teliosporas de *Ustilago scitaminea*

Sydow en yemas de la caña de azúcar (*Saccharum* sp.). Rev Biol 13:141–144

del Monte-Martínez A, González-Bacerio J, Aragón-Abreu C, Palomo-Carmona JM, Guisán-Seijas JM, Díaz-Brito J (2012) Selective and oriented immobilization of (phospho)lipases from the Caribbean Sea anemone *Stichodactyla helianthus* (Ellis, 1768) by interfacial adsorption. Rev CENIC Cien Biol 43:3–8

del Monte-Martínez A, Cutiño-Avila B, González-Bacerio J, Chávez MÁ, Díaz J (2014) Rational design of protein immobilization: applications on affinity chromatography and enzymatic bioconversion. Anal Acad Cien Cuba 4:1–15

del Monte-Martínez A, González-Bacerio J, Cutiño-Avila B, Ruiz R, Avila R, Ramos-Leal M, Nolasco H, Díaz J, Guisán JM (2015) Esters biotransformation by immobilized interfacial esterases from the Caribbean Sea anemone *Stichodactyla helianthus*. Biotecnol Appl 32:3201–3210

del Monte-Martínez A, González-Bacerio J, Cutiño-Avila B, Rojas J, Chappé M, Salas-Sarduy E, Pascual I, Guisán JM (2017) Rational design and synthesis of affinity matrices based on proteases immobilized onto cellulose membranes. Prep Biochem Biotechnol 47:745–753. https://doi.org/10.1080/10826068.2017.1315600

del Monte-Martínez A, Cutiño-Avila BV, González-Bacerio J (2018) Rational design strategy as a novel immobilization methodology applied to lipases and phospholipases. In: Sandoval G (ed) Lipases and phospholipases: methods and protocols, Meth mol biol, vol 1835. Springer Science + Business Media. LLC, New York, pp 243–283

del Monte-Martínez A, Cutiño-Avila B, González-Bacerio J, Chávez MÁ, Díaz J, Guisán JM (2019) Modelado in silico de derivados inmovilizados. In: Chávez MÁ, Díaz J, Arias O (eds) Nano-microbiotecnologías y sus aplicaciones. Editorial UH, La Habana, pp 155–180

Duca D, Lorv J, Patten CL, Rose D, Glick BR (2014) Indole-3-acetic acid in plant-microbe interactions. Antonie Van Leeuwenhoek 106:85–125. https://doi.org/10.1007/s10482-013-0095-y

Eş I, Khaneghah AM, Barba FJ, Saraiva JA, Sant'Ana AS, Hashemi SMB (2018) Recent advancements in lactic acid production—a review. Food Res Int 107:763–770. https://doi.org/10.1016/j.foodres.2018.01.001

Fosso-Kankeu E, Mulaba-Bafubiandi AF, Barnard TG (2014) Establishing suitable conditions for metals recovery from metal saturated *Bacillaceae* bacterium using experimental design. Int Biodet Biodeg 86:218–224. https://doi.org/10.1016/j.ibiod.2013.09.022

Glickmann E, Dessaux Y (1995) A critical examination of the specificity of the Salkowski reagent for indolic compounds produced by phytopathogenic bacteria. Appl Environ Microbiol 61:793–796

Guisán JM (2006) Immobilization of enzymes and cells. Meth biotechnol, 2nd edn. Humana Press Inc, Totowa, New Jersey

Guisán JM (2013) Immobilization of enzymes and cells. Methods in molecular biology. Humana Press Inc, Totowa, New Jersey

Héctor E, Rodríguez R, de Prada F, del Monte-Martínez A, González R (1995) Experimental evidence for the presence of different smut resistance mechanism in sugar cane. In: Napompeth B (ed) Proceedings XXI Congress International Society of Sugar Cane Technologists (ISSCT), 5-14 March 1992, Bangkok, Thailand, vol 2. Kasetsart University Press, Bangkok, pp 565–575

Hyland SA, Eveland SS, Anderson MS (1997) Cloning, expression, and purification of UDP-3-O-acyl-GlcNAc deacetylase from *Pseudomonas aeruginosa*: a metalloamidase of the lipid A biosynthesis pathway. J Bacteriol 179:2029–2037. https://doi.org/10.1128/jb.179.6.2029-2037.1997

Idris EE, Iglesias DJ, Talon M, Borriss R (2007) Tryptophan-dependent production of indole-3-acetic acid (IAA) affects level of plant growth promotion by *Bacillus amyloliquefaciens* FZB42. MPMI 20:619–626. https://doi.org/10.1094/MPMI-20-6-0619

Infante PF, Schuman LD, Huff J (1996) Fibrous glass insulation and cancer: response and rebuttal. Am J Ind Med 30:113–120. https://doi.org/10.1002/(sici)1097-0274(199607)30:1%3c113:aid-ajim21%3e3.0.co;2-%23

Khandaker MM, Azam HM, Rosnah J, Tahir D, Nashriyah M (2018) The effects of application of exogenous IAA and GA_3 on the physiological activities and quality of *Abelmoschus esculentus* (Okra) var. Singa 979. Pertanika J Trop Agric Sci 41:209–224

Kohler T, Weidenmaier C, Peschel A (2009) Wall teichoic acid protects *Staphylococcus aureus* against antimicrobial fatty acids from human skin. J Bacteriol 191:4482–4484. https://doi.org/10.1128/JB.00221-09

Kumar R, Vats R (2010) Protease production by *Bacillus subtilis* immobilized on different matrices. New York Sci J 3:20–24

Kwon K, Hasseman J, Latham S, Grose C, Do Y, Fleischmann RD, Pieper R, Peterson SN (2011) Recombinant expression and functional analysis of proteases from *Streptococcus pneumoniae, Bacillus anthracis, and Yersinia pestis*. BMC Biochem 12:17. https://doi.org/10.1186/1471-2091-12-17

Labra-Cardón D, Guerrero-Zúñiga LA, Rodríguez-Tovar AV, Montes-Villafán S, Pérez-Jiménez S, Rodríguez-Dorantes A (2012) Respuesta de crecimiento y tolerancia a metales pesados de *Cyperus elegans* y *Echinochloa polystachya* inoculadas con una rizobacteria aislada de un suelo contaminado con hidrocarburos derivados del petróleo. Rev Int Contam Ambie 28:7–16

Lambe TW, Whitman RV (2007) Mecánica de suelos. Editorial Limusa, Mexico

Madigan M, Martinko JM, Stahl DA, Clark DP (2012) Brock biology of microorganisms, 13th edn. Pearson Education Inc., San Francisco

Martínez D, Cutiño-Avila B, Pérez ER, Menéndez C, Hernández L, del Monte-Martínez A (2014) A thermostable exo-β-fructosidase immobilised through rational design. Food Chem 145:826–831. https://doi.org/10.1016/j.foodchem.2013.08.073

Medeiros AA, O'Brien TF, Wacker WE, Yulug NF (1971) Effect of salt concentration on the apparent in vitro susceptibility of *Pseudomonas* and other gram-negative bacilli to gentamicin. J Infect Dis 124:S59–64. https://doi.org/10.1093/infdis/124.supplement_1.s59

Menéndez C, Martínez D, Trujillo LE, Ramírez R, Sobrino A, Cutiño-Ávila BV, Basabe L, del Monte-Martínez A, Pérez ER, Hernández L (2014) Development of soluble and immobilized biocatalysts based on a recombinant thermostable β-fructosidase enabling complete sucrose inversion at pasteurization temperatures. Biotecnol Appl 31:249–253

Natural Committee for Clinical Laboratory Standards (NCCLS) (2005) Performance standards for antimicrobial disk. Susceptibility test, Approved standard, p 238

Nazhmetdinova A, Sarmanbetova G, Magai A (2018) The characteristics of pollution in the big industrial cities of Kazakhstan by the example of Almaty. J Environ Health Sci Engin 16:81–88. https://doi.org/10.1007/s40201-018-0299-1

Orts MJ, Campos B, Picó M, Gozalbo K (2014) Métodos de análisis granulométrico. Aplicación al control de la granulometría de materias primas. Instituto de Tecnología Certimica, Universitat Jaume 1, Castellón, Asociación de Investigación de las Industrias Cerámicas (AICE), Castellón, Spain

Palazon J, Bonfil M, Cusido RM, Pinol MT, Morales M (1995) Effects of auxin and phenobarbital on morphogenesis and production of digitoxin in *Digitalis callus*. Plant Cell Phisiol 36:247–252. https://doi.org/10.1093/oxfordjournals.pcp.a078756

Pini F, Galardini M, Bazzicalupo M, Mengoni A (2011) Plant-bacteria association and symbiosis: are there common genomic traits in *Alphaproteobacteria*? Genes 2:1017–1032. https://doi.org/10.3390/genes2041017

Plou FJ, Sandoval G (2012) Obtención enzimática de compuestos bioactivos a partir de recursos naturales iberoamericanos. Colección Biblioteca de Ciencias, vol 40, Editorial CSIC, CSIC, Madrid

Rajneesh Singh SP, Pathak J, Sinha RP (2017) Cyanobacterial factories for the production of green energy and value-added products: an integrated approach for economic viability. Renew Sustain Energ Rev 69:578–595. https://doi.org/10.1016/j.rser.2016.11.110

Rogers CA (1947) Existence theorems in the geometry of numbers. Annal Math 2nd Ser 48:994–1002. https://doi.org/10.2307/1969390

Salager JL (2007) Granulometría teórica. Cuaderno FIRP S554-A. Universidad de los Andes, Mérida, Venezuela 312:98–107

Salgado-Bernal I, Pérez JE, Carballo ME, Martínez A, Cruz M (2015) Aplicación de rizobacterias en la biorremediación del cromo hexavalente presente en aguas residuals. Rev Cub Cienc Biol 4:20–34

Sandoval G (ed) (2012) Lipases and phospholipases: methods and protocols. Meth mol biol, vol 861. Springer Science + Business Media, LLC, New York

Sethi S, Kumar R, Gupta S (2013) Antibiotic production by microbes isolated from soil. Int J Pharm Sci Res 4:2967–2973

Snedecor GW, Cochran WG (1989) Statistical methods, 8th edn. Iowa State University Press, Iowa

Steffan S, Bardi L, Marzona M (2005) Azo dye biodegradation by microbial cultures immobilized in alginate beads. Environ Int 31:201–205. https://doi.org/10.1016/j.envint.2004.09.016

Thatoi H, Das S, Mishra J, Rath BP, Das N (2014) Bacterial chromate reductase, a potential enzyme for bioremediation of hexavalent chromium: a review. J Environ Manage 146:383–399. https://doi.org/10.1016/j.jenvman.2014.07.014

Torres-Rubio MG, Valencia-Plata SA, Bernal-Castillo J, Martínez P (2000) Isolation of enterobacteria, *Azotobacter* sp. and *Pseudomonas* sp., producers of indol-3-acetic acid and siderophores, from Colombian rice rhizosphere. Rev Lat Microbiol 42:171–176

Tukey J (1949) Comparing individual means in the analysis of variance. Biometrics 5:99–114. https://doi.org/10.2307/3001913

Verstrepen KJ, Derdelinchkx G, Verachtert Y, Delvaux FR (2003) Yeast flocculation: what brewers should know. Appl Microbiol Biotechnol 61:197–205. https://doi.org/10.1007/s00253-002-1200-8

Vincent MC, Zaragoza JL, Blanco SA (2006) Química industrial orgánica. Universidad Politécnica de Valencia, Valencia

Wassel MA, Swelam AA, El-Zaref AS (2013) Comparative adsorption of cadmium Cd(II) ions using anion exchanger Amberjet 4200 Cl from aqueous - mineral acids and aqueous - organic acids media. J Appl Sci Res 9:5097–5111

Weidenmaier C, Kokai-Kun JF, Kulauzovic E, Kohler T, Thumm G, Stoll H, Gotz F, Peschel A (2008) Differential roles of sortase-anchored surface proteins and wall teichoic acid in *Staphylococcus aureus* nasal colonization. Int J Med Microbiol 298:505–513. https://doi.org/10.1016/j.ijmm.2007.11.006

Willaert RG (2006) Cell immobilization and its applications in biotechnology: current trends and future prospects. In: El-mansi EMT, Bryce CFA, Demain AL, Allman AR (eds) Fermentation microbiology and biotechnology, 2nd edn. CRC Press, FL, pp 289–362

Woodward J (1988) Methods of immobilization of microbial cells. J Microbiol Meth 8:91–102. https://doi.org/10.1016/0167-7012(88)90041-3

Zhang P, Jin T, Sahu SK, Xu J, Shi Q, Liu H, Wang Y (2019) The distribution of tryptophan-dependent indole-3-acetic acid synthesis pathways in bacteria unraveled by large-scale genomic analysis. Molecules. https://doi.org/10.3390/molecules24071411

Zinicovscaia I (2012) A review on biosorption of chromiun ions by microorganisms. Chem J Mold 7:27–31